

# Detection of DNA Targets Hybridized to Solid Surfaces Using Optical Images of Liquid Crystals

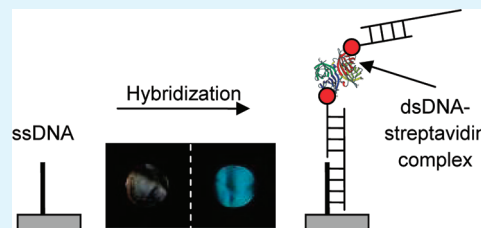
Siok Lian Lai, Wei Ling Tan, and Kun-Lin Yang\*

Department of Chemical and Biomolecular Engineering, National University of Singapore, 4 Engineering Drive 4, Singapore 117576

Supporting Information

**ABSTRACT:** In this paper, we report a method of detecting DNA targets hybridized to a solid surface by using liquid crystals (LC). The detection principle is based on different interference colors of LC supported on surfaces decorated with single-stranded DNA (ssDNA) or double-stranded DNA (dsDNA). However, the contrast between the ssDNA and dsDNA is not obvious, unless DNA-streptavidin complexes are introduced to the dsDNA to increase the surface mass density. Two different approaches of introducing streptavidin to the system are studied and compared. We find that by premixing the biotin-labeled DNA targets with streptavidin prior to the DNA hybridization, branched-streptavidin complexes are formed and clear LC signal can be observed. This LC-based DNA detection principle represents an important step toward the development of a simple, instrument- and fluorophore-free DNA detection method.

**KEYWORDS:** liquid crystals, DNA microarray, DNA targets detection, single-stranded DNA, double-stranded DNA, Biotin, Streptavidin



## INTRODUCTION

Detection of DNA target with specific sequences has become increasingly important in the identification of single nucleotide polymorphisms and gene expression analysis.<sup>1–4</sup> Among various detection methods, DNA microarrays have been used extensively due to its high throughput nature, which allows the simultaneous detection of few thousand of DNA targets at one time. A DNA microarray often features immobilized DNA probes on a solid surface and followed by the hybridization of fluorescently labeled DNA targets.<sup>5–7</sup> However, traditional DNA microarray requires the labeling of DNA targets with fluorophores, which may degrade over time because of photobleaching.<sup>8,9</sup> Although some label-free detection methods such as surface plasmon resonance (SPR) and ellipsometry have been used to detect label-free DNA targets hybridize to solid surfaces,<sup>10–12</sup> these methods are not compatible with DNA microarray because they require a reflective surface and the scan area is not large enough for a normal DNA microarray slide. Furthermore, they require additional instrumentation which is bulky and not feasible for point-of-care applications. In view of this, we explore the feasibility of using thermotropic liquid crystals (LC) as a simple and instrument-free method to detect the DNA targets hybridize to solid surfaces.

In the past decade, it has been reported in several studies that a thin layer of LC supported on a solid surface can be used as a powerful imaging tool to probe the chemical functionality of the surface.<sup>13–22</sup> Advantages of the LC method include simplicity and high spatial resolution. For example, Tingey et al. showed that a thin layer of LC supported on a gold surface decorated with square protein patterns displays a matching color pattern under crossed polars.<sup>15</sup> Recently, we also developed an LC-based imaging tool to examine the quality of single-stranded DNA

(ssDNA) spots on solid surfaces.<sup>20</sup> It was shown that when the surface density of immobilized ssDNA probes exceeds a critical value, the homeotropic orientation of LC is disrupted and that led to a distinct bright spot on a dark background. However, in the previous work, we only studied the interactions of LC with ssDNA covalently immobilized on the surface. In a separate work by Kim et al, they studied the interactions of LC with both ssDNA and dsDNA, and found that LC supported on solid surfaces decorated with ssDNA appears dark while LC supported on solid surfaces decorated with dsDNA appears bright.<sup>17</sup> Apparently, their conclusion of how ssDNA dictates the orientations of LC is different from ours, probably because of different DNA immobilization strategies used. Despite the promise of their method in differentiating ssDNA and dsDNA, they did not test the specificity for DNA with different sequences. Recently, Price et al. utilized an LC-aqueous interface to study DNA hybridization.<sup>23</sup> In this system, ssDNA adsorbed on the surfactant-laden interface caused LC to appear bright under crossed polars. After the addition of complementary DNA targets to the aqueous solution and the formation of dsDNA, some dark domains in the LC are observed. The method is capable of discriminating 1-base pair mismatch DNA targets at a very low concentration ( $\sim 50$  fmol). Later, we used a similar platform to detect DNA targets through the use of surface-active cholesterol-labeled ssDNA probes.<sup>24</sup> The system is able to discriminate complementary from the non-complementary DNA targets and the changes of LC optical image can be observed within 15 min. These LC-aqueous interface systems are good for real-time and fast detection, but they are not

Received: May 9, 2011

Accepted: August 8, 2011

Published: August 23, 2011

compatible with high throughput DNA microarray technology because of the lack of a solid surface in this design.

Herein, we study the orientations of LC supported on surfaces decorated with ssDNA and dsDNA, and investigate strategies to improve the contrast between ssDNA and dsDNA by introducing DNA–protein complexes to the system. This study is motivated by difficulties encountered in our previous investigation on the interactions between LC and ssDNA. It was found that LC supported on ssDNA does not give a uniform optical image as compared to LC supported on proteins.<sup>20,21</sup> One of the differences between DNA and proteins is their size. Because of DNA's smaller size, DNA cannot disrupt LC easily like proteins. Thus, to produce a pronounced and uniform optical image in the LC assay, we designed DNA–protein complexes to increase the size of DNA. We hypothesize that the larger size of the DNA complex can disrupt the orientations of LC more easily. In this study, we chose streptavidin as a model to complex with biotin-labeled DNA because streptavidin can bind to biotin with high affinity (dissociation constant of  $K_d \approx 1 \times 10^{-15}$  M).<sup>25</sup>

## EXPERIMENTAL SECTION

**Materials.** Microscope glass slides (Fisher's Finest) were purchased from Fisher (U.S.A.). *N,N*-dimethyl-*n*-octadecyl-3-aminopropyltrimethoxysilyl chloride (DMOAP) and sodium cyanoborohydride ( $\text{NaBH}_3\text{CN}$ ) were purchased from Sigma Aldrich (Singapore). Streptavidin-Cy3 was purchased from Invitrogen (Singapore). (Triethoxysilyl) butyl aldehyde (TEA) was purchased from United Chemical Technologies (U.S.A.). LC, 4-cyano-4'-pentylbiphenyl (5CB), was purchased from Merck (Singapore). DNA probes 5'-NH<sub>2</sub>-GTGGC TCGAT ATAAT ATGCA AAAGC-3' (**P**<sub>1</sub>), 5'-NH<sub>2</sub>-GTGGC TCGAT ATAAT ATGCA AAAGC-biotin-3' (**biotin-P**<sub>1</sub>), 5'-NH<sub>2</sub>-CTGCA TGTC TGGTA CTAAG CCTGA-3' (**P**<sub>2</sub>), and DNA targets, 5'-GCTTT TGCAT ATTAT ATCGA GCCAC-3' (**T**<sub>1</sub>), 5'-Cy3-GCTTT TGCAT ATTAT ATCGA GCCAC-3' (**T**<sub>1</sub>-Cy3), 5'-CACCG AGCTA TATTA TACGT TTTTCG GCTTT TGCAT ATTAT ATCGA GCCAC-3' (**T**<sub>2</sub>), and 5'-CGAAA ACGTA TAATA TAGCT CGGTG-biotin-3' (**biotin-P**<sub>3</sub>) used in this study were purchased from Sigma Aldrich (Singapore).

**Preparation of Mixed DMOAP/TEA-Coated Surface.** The DMOAP/TEA-coated surface can be prepared following our procedure published previously.<sup>20</sup> Briefly, microscope glass slides were immersed in a 5% Decon-90 solution overnight. This was followed by sonicating in DI water and rinsed thoroughly with DI water. The cleaned glass slides were then immersed in an aqueous solution containing 0.1% (v/v) DMOAP for 1 min. The glass slides were rinsed with copious amounts of DI water, dried under nitrogen and heated in a 100 °C vacuum oven for 15 min. After this, the DMOAP-coated glass slides were immersed in a methanolic solution containing 3% (v/v) TEA for 4 h. The mixed DMOAP/TEA-coated glass slides were rinsed with methanol, dried under nitrogen, and heated in a 100 °C vacuum oven for 15 min. The mixed DMOAP/TEA-coated glass slides were used immediately for DNA immobilization.

**Preparation of Solid Surfaces Decorated with ssDNA.** To immobilize amine-labeled ssDNA on a mixed DMOAP/TEA-coated surface, we used 20 mM of Tris buffer (pH 8.5) containing 100 mM of  $\text{MgCl}_2$  and 50 mM of  $\text{NaBH}_3\text{CN}$  to dissolve DNA probes (**P**<sub>1</sub>, **biotin-P**<sub>1</sub> or **P**<sub>2</sub>). The DNA solution was spotted onto the solid surfaces with a spotting robot (Biodot, U.S.A.). The diameter of each spot was 0.8 mm and the distance between two spots was 1.5 mm. Humidity was maintained at 90% during the spotting process. After 18 h of incubation in a humid chamber, the slides were sonicated in methanol solution for 2 min. The slides were then incubated in 2 × SSPE buffer (pH 7.4) containing 0.2% of SDS for 4 h to remove any nonspecifically adsorbed

DNA probes. After the incubation, the slides were washed with the same incubation buffer twice (5 min each). After washing and drying with the nitrogen, the slides were ready for subsequent experiments. To estimate the surface density of immobilized ssDNA probes, we spotted Cy3-labeled ssDNA with a concentration range between 0.01 nM and 5  $\mu\text{M}$  on the mixed DMOAP/TEA-coated surfaces and let the spots dry up completely. The slides were scanned with a fluorescence scanner and a calibration curve between the fluorescence intensity and total number of ssDNA on the surface was established. Next, 1  $\mu\text{M}$  of Cy3-labeled ssDNA was immobilized on the solid surface. After washing, the fluorescence intensity was scanned, measured and compared to the calibration curve. By using this method, the estimated the surface density of 5 and 1  $\mu\text{M}$  ssDNA probes on mixed DMOAP/TEA surface is about  $4.00 \times 10^{12}/\text{cm}^2$  and  $3.22 \times 10^{12}/\text{cm}^2$  respectively.

**Preparation of Solid Surfaces Decorated with dsDNA.** Solid surfaces decorated with ssDNA probes were incubated in 2 × SSPE buffer containing 0.2% of SDS and 5  $\mu\text{M}$  of DNA targets (**T**<sub>1</sub>) underneath a Lifter slip (Erie Scientific, U.S.A.). After DNA hybridization for 4 h, the slides were washed with the same hybridization buffer twice (5 min each).

**Preparation of Solid Surfaces Decorated with DNA-Streptavidin Complexes.** First, 2 × SSPE buffer containing 0.2% of SDS, 5  $\mu\text{M}$  of **T**<sub>2</sub>, and 5  $\mu\text{M}$  of **biotin-P**<sub>3</sub> were mixed for 1 h. The time is required to ensure that one end of **T**<sub>2</sub> hybridized to **biotin-P**<sub>3</sub>. Second, solid surfaces decorated with ssDNA probes were incubated in this DNA solution for 4 h, allowing the hybridization between **T**<sub>2</sub> and DNA probes. Finally, the slides were washed with 2 × SSPE buffer containing 0.2% of SDS twice (5 min each). The slides were then incubated in PBS buffer (pH 7.0) containing 0.19  $\mu\text{M}$  of streptavidin-Cy3 and 0.1% Tween 20 under a Lifter slip. After 1 h, the slides were sequentially washed with PBS buffer (with 0.1% SDS) once and PBS buffer (without SDS) twice (1 min each). In other experiment, 2 × SSPE buffer containing 0.2% of SDS, 5  $\mu\text{M}$  of **T**<sub>2</sub>, 5  $\mu\text{M}$  of **biotin-P**<sub>3</sub> and 0.19  $\mu\text{M}$  of streptavidin-Cy3 were mixed for 1 h to allow **T**<sub>2</sub> hybridized to **biotin-P**<sub>3</sub> and the conjugation of biotin-streptavidin complexes. Then, solid surfaces decorated with ssDNA probes were incubated in this branched DNA-streptavidin complexes (**T**<sub>2</sub>/**biotin-P**<sub>3</sub>/streptavidin) solution for 4 h, allowing the hybridization between **T**<sub>2</sub> and DNA probes. Finally, the slides were washed with 2 × SSPE buffer containing 0.2% of SDS twice (5 min each). This vigorous rinsing procedure was shown to remove the nonspecific adsorbed DNA and proteins on surfaces.<sup>18,26</sup>

**Fluorescence Detection.** The glass slides were scanned by using a microarray scanner GenePix 4100A (Molecular Devices, U.S.A.) with a 575DF35 bandpass filter (550–600 nm). The spatial resolution was maintained at 40  $\mu\text{m}$  and the PMT gain used was 450 in all experiments. All images were analyzed by using GenePix Pro 6.1 provided by the manufacturer. To ensure the reproducibility and minimize the errors of the fluorescent measurement, we measured three different spots from three replicates and the fluorescence intensity was averaged. Calibration of the scanner was carried out by using the hardware diagnostic tool in GenePix Pro 6.1 to scan a calibration slide provided by the manufacturer.

**Fabrication of Liquid Crystal (LC) Cell.** A LC cell was fabricated by sandwiching two glass slides, one was a DMAOP-coated slide and the other was a DMOAP/TEA-coated slide decorated with either ssDNA or dsDNA. These two slides were separated by using two strips of spacer ( $\sim 6 \mu\text{m}$ ) and secured with two binder clips. The DMOAP-coated slide was used because it is known to cause homeotropic orientations of LC.<sup>27,28</sup> Approximately 3  $\mu\text{L}$  of 5CB was drawn into the cavity formed between the two solid surfaces through capillary force. The optical image of the cell was observed by using a polarizing optical microscope (Nikon, Japan) in transmission mode. Each image was captured by a digital camera mounted on the microscope using an exposure time of 1/40 s.

## RESULTS AND DISCUSSIONS

**Optical Images of LC on Surfaces Decorated with ssDNA and dsDNA.** We first compared the optical images of LC supported on surfaces with and without ssDNA. Figure 1a shows that the optical image of LC within the circular region decorated with  $5 \mu\text{M}$  of ssDNA ( $P_1$ ) is in light orange color. In contrast, LC in the surrounding area free of ssDNA appears dark. This suggests that the immobilized ssDNA on the solid surface disrupts the homeotropic orientations of LC and causes the LC color to turn bright. This is in good agreement with our previous study in which the LC showed bright color when the ssDNA concentration used was above  $0.5 \mu\text{M}$ .<sup>20,29</sup> Next, we compared the optical image of LC supported on surfaces decorated with ssDNA ( $P_1$ ) and dsDNA ( $P_1/T_1$ ). Because the dsDNA has a higher DNA density than ssDNA, we anticipate that the interference color of LC will be more colorful.<sup>20</sup> However, Figure 1b shows that the dsDNA spot shows similar interference color as ssDNA. This implies that the surface density of dsDNA is similar to ssDNA. By using fluorescence intensity, we determined that the DNA hybridization efficiency on the dsDNA spots in Figure 1b is only 28%, which is relatively low compared to 100% hybridization efficiency reported by others.<sup>30</sup>

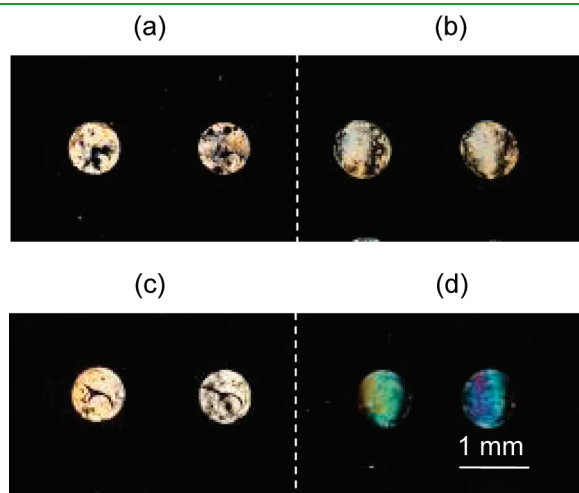


**Figure 1.** Comparison of optical images of the LC supported on surfaces decorated with different DNA probes. (a) ssDNA  $P_1$ , (b) dsDNA  $P_1/T_1$ , (c) ssDNA **biotin- $P_1$** , and (d) ssDNA streptavidin complex. Concentrations of all DNA probes during immobilization are  $5 \mu\text{M}$ .

The low hybridization efficiency of our system as compared to others is probably due to the different hybridization procedure (such as the concentration of DNA targets, salt concentration in the hybridization buffer, hybridization temperature and duration) used. As such, our result shows that LC is not sensitive enough to detect an increase of 28% in DNA surface density.

**LC Supported on Biotin-Labeled DNA.** Because the optical images of LC supported on ssDNA and dsDNA cannot be differentiated, we hypothesize that the contrast between ssDNA and dsDNA will be increased if the target DNA is conjugated to a protein. This hypothesis is constructed based on a series of past studies showing that the interference color of LC is affected by the amount of proteins adsorbed on the surface.<sup>19,20</sup> To test this hypothesis, we first immobilized biotin-labeled ssDNA (**biotin- $P_1$** ) on glass slides. Some of the samples were further incubated in an aqueous solution containing  $0.19 \mu\text{M}$  of streptavidin (SAV), allowing the binding of streptavidin to the biotin label. Successful binding of streptavidin was confirmed by using fluorescence microscopy (data not shown). Next, we compared the optical images of LC supported on biotin-labeled ssDNA with and without conjugated to streptavidin. Figure 1c shows that LC in the circular region decorated with  $5 \mu\text{M}$  of biotin-labeled DNA gives light orange color, similar to that of ssDNA in Figure 1a. This indicates that the additional biotin tag has negligible effect on the LC. In contrast, Figure 1d shows that the LC in the circular region decorated with biotin-labeled ssDNA conjugated to streptavidin exhibits blue-green color. As shown in the Michel-Levy chart (see the Supporting Information), the order of blue-green interference color is higher than that of the light orange color.<sup>31</sup> This suggests that the presence of biotin-streptavidin conjugate effectively increases the disruption of LC and causes a more obvious interference color.

It is believed that the driving force for the disruption of the orientations of LC by the DNA/streptavidin conjugate is the surface energy. After the introduction of DNA/streptavidin on the surface, the DNA/streptavidin spots became more hydrophilic as compared to the surrounding surface. As reported by our group and other groups before, LC molecules assume homeotropic orientations on hydrophobic surface and planar/disrupted orientations on hydrophilic surface.<sup>20,32</sup> Besides, molecules in the LC phase can communicate their orientations up to  $100 \mu\text{m}$  away from the surface.<sup>13</sup> Thus, even though the DNA/streptavidin layer is in nanometer thickness, this information can be amplified through

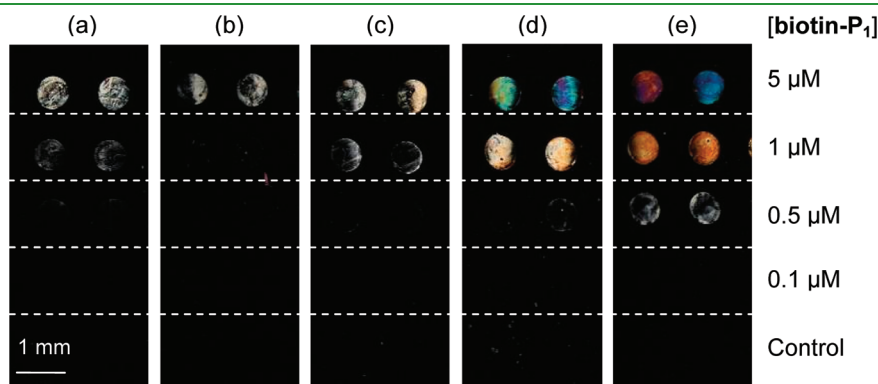


**Figure 2.** Effect of DNA surface density and streptavidin concentration on the optical image of LC. Different concentrations of **biotin- $P_1$**  (as indicated) were immobilized on glass slides. The glass slides were incubated in different concentrations of streptavidin for 1 h. The concentrations of streptavidin used were (a)  $0.19 \text{ nM}$ , (b)  $1.9 \text{ nM}$ , (c)  $0.019 \mu\text{M}$ , (d)  $0.19 \mu\text{M}$ , and (e)  $1.9 \mu\text{M}$ .

the 6  $\mu\text{m}$  thick LC layer and appear as different interference color for different surface density.

**Effect of the Streptavidin Concentration.** Since the use of biotin-streptavidin conjugate shows promise to increase the interference color of LC, we further studied how the interference color of LC changes with the concentration of streptavidin. In this experiment, slides decorated with dots of biotin-labeled ssDNA (**biotin-P<sub>1</sub>**) were first immersed into streptavidin solutions with concentrations between 0.19 nM and 1.9  $\mu\text{M}$ . After rising and drying, LC cells were made from these slides. Figure 2 shows that, when the streptavidin concentration is increased from 0.19 nM to 1.9  $\mu\text{M}$ , the optical image of the 5  $\mu\text{M}$  **biotin-P<sub>1</sub>** dots (first row) gradually changes from white-gray color to blue color, whereas the optical image of the 1  $\mu\text{M}$  **biotin-P<sub>1</sub>** dots (second row) gradually changes from dark to orange color. The changes of LC interference color with increasing streptavidin concentration are in accordance with the increasing surface density of biotin-streptavidin conjugate as shown in Figure 3. In addition, Figure 2 shows that when the **biotin-P<sub>1</sub>** concentration is 0.5  $\mu\text{M}$  and below (the third and fourth rows), the spots appear as dark for all streptavidin concentrations studied. These

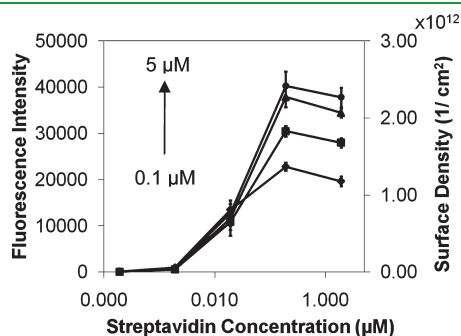


**Figure 3.** Effect of streptavidin and DNA concentrations on the surface density of biotin-streptavidin conjugate (measured by using fluorescence intensity). DNA concentrations from low to high are 0.1, 0.5, 1, and 5  $\mu\text{M}$ , respectively.

results, when combined, suggest that both biotin-DNA and streptavidin concentrations affect the interference colors. The minimum biotin-DNA and streptavidin concentrations required to cause bright LC image are 1  $\mu\text{M}$  and 0.19  $\mu\text{M}$ , respectively. Under this condition, the surface densities of **biotin-P<sub>1</sub>** and streptavidin are  $3.22 \times 10^{12}/\text{cm}^2$  and  $2.35 \times 10^{12}/\text{cm}^2$ , respectively. Thus, we can estimate that the binding ratio of streptavidin to **biotin-P<sub>1</sub>** of about 1.4. This is in agreement with a biotin-to-streptavidin ratio of 1.5 reported earlier.<sup>33</sup>

**Label-Free Detection of DNA Targets Using Biotin-Streptavidin DNA Probes.** Next, we studied whether the biotin-streptavidin system can be used to detect DNA targets hybridize on solid surface with better contrast. To avoid labeling our DNA target **T<sub>2</sub>** with a biotin (for label-free detection), we design a new probe **biotin-P<sub>3</sub>** to hybridize with **T<sub>2</sub>**. A schematic of the detection procedure is shown in Figure 4a. First, **T<sub>2</sub>** is premixed with **biotin-P<sub>3</sub>**, allowing the hybridization of **T<sub>2</sub>** and **biotin-P<sub>3</sub>**. The 5' end of **T<sub>2</sub>** has 25-mer bases, which are complementary to **biotin-P<sub>3</sub>**. The slide decorated with **P<sub>1</sub>** was then immersed into the solution to allow the hybridization of the 3' end of **T<sub>2</sub>**. At the end of the hybridization, the slide was rinsed briefly and then transferred to PBS buffer containing 0.19  $\mu\text{M}$  of streptavidin-Cy3 and 0.1% Tween 20 to form a DNA-streptavidin complex on the surface as shown in Figure 4a. Fluorescence images also confirm the presence of the DNA-streptavidin complexes and the stability of the biotin-streptavidin conjugates formed on the surface (data not shown). When we observed the LC cell made from the slide, two blue-orange spots can be seen (Figure 5a). These colorful spots suggest the formation of a complex involving **P<sub>1</sub>**, **T<sub>2</sub>**, and **biotin-P<sub>3</sub>** disrupt LC orientations. For comparison, we also conducted several control experiments in which we removed either **T<sub>2</sub>**, (Figure 5b), **biotin-P<sub>3</sub>** (Figure 5c) or streptavidin (Figure 5d). In the absence of **T<sub>2</sub>**, **biotin-P<sub>3</sub>** cannot hybridize to **P<sub>1</sub>**. In this case, only ssDNA is present on the surface and that leads to a gray spot (Figure 5b). Similarly, in the absence of **biotin-P<sub>3</sub>** or streptavidin, only dsDNA is present on the surface. Therefore, LC exhibits higher interference color order than that in Figure 5b, but lower than that in Figure 5a because of the lack of

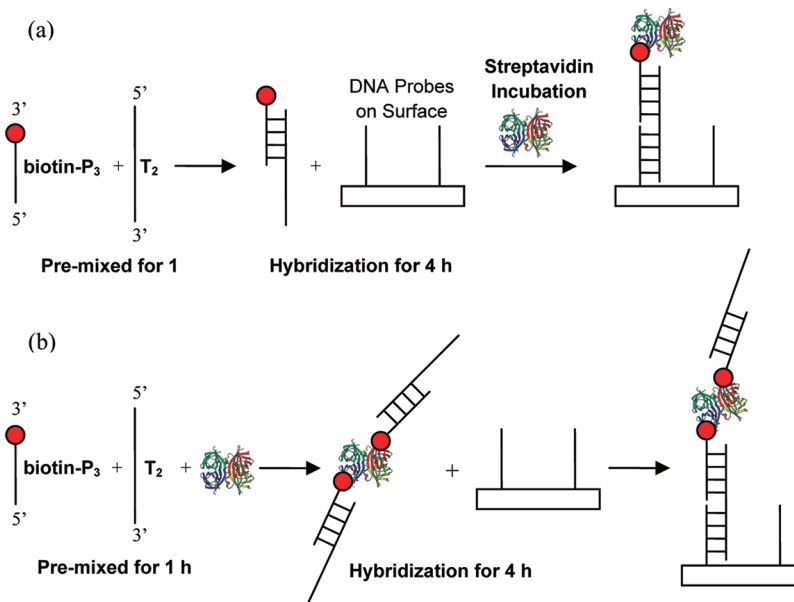


**Figure 4.** Schematic illustration of the (a) single-biotin-streptavidin conjugates and (b) branched-streptavidin complexes system. Drawings are not to scale.

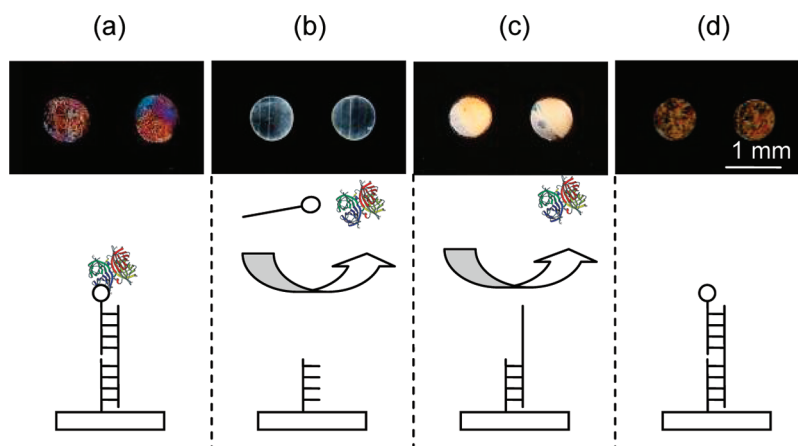


**Figure 5.** LC image shows the  $1 \mu\text{M}$  of  $\text{P}_1$  spots hybridized with (a) biotin- $\text{P}_3/\text{T}_2/\text{SAv}$  conjugates; (b) biotin- $\text{P}_3$ , which are not complementary to  $\text{P}_1$ ; and (c)  $\text{T}_2$  DNA targets. The slides were incubated in streptavidin after the DNA hybridization. (d)  $1 \mu\text{M}$  of  $\text{P}_1$  spots were hybridized with biotin- $\text{P}_3/\text{T}_2$  without the incubation of streptavidin. The DNA hybridization was illustrated in the scheme underneath each figure. Drawings are not to scale.

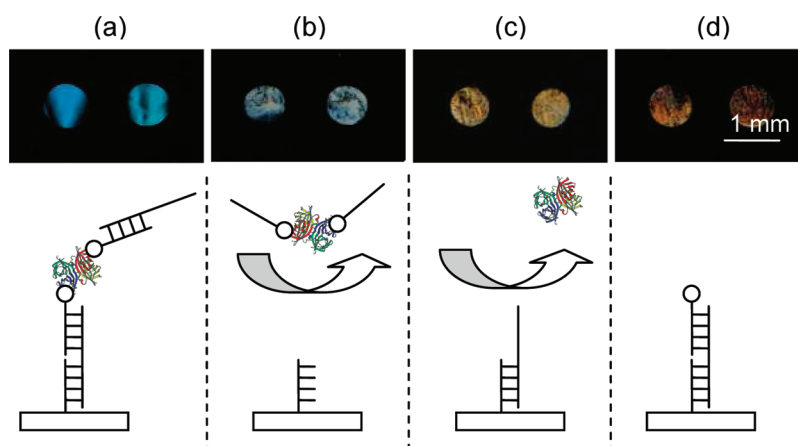


**Figure 6.** LC image shows the  $1 \mu\text{M}$  of  $\text{P}_1$  spots hybridized with (a) biotin- $\text{P}_3/\text{T}_2/\text{SAv}$ , (b) biotin- $\text{P}_3/\text{SAv}$ , (c)  $\text{T}_2/\text{SAv}$ , and (d) biotin- $\text{P}_3/\text{T}_2$  without streptavidin according to the scheme in Figure 4B. The DNA hybridization was illustrated in the scheme underneath each figure. Drawings are not to scale.

streptavidin. Details regarding the analysis of the order of interference color can be found in the Supporting Information. These results, when combined, suggest that all three components ( $\text{P}_1$ ,  $\text{T}_2$ , and biotin- $\text{P}_3$ ) are important to disrupt LC for giving interference color in the higher order.

We also studied whether it is possible to prepare a cocktail solution containing streptavidin,  $\text{T}_2$  and biotin- $\text{P}_3$  before DNA hybridization (Figure 4b). Because streptavidin has four binding sites for biotin, when streptavidin and biotin-labeled DNA are mixed together, 4 types of DNA-streptavidin complexes (with 1 to 4 biotin-labeled DNA) can be formed rapidly in the solution.<sup>34,35</sup> Past studies have shown that dibiotin-streptavidin complexes make up the major component in order to maintain the stability of the streptavidin complexes.<sup>34</sup> Figure 6a shows that the LC on  $\text{P}_1/\text{T}_2/\text{biotin-P}_3/\text{SAv}$  complex spots is in blue color. In contrast, when we removed  $\text{T}_2$ , biotin- $\text{P}_3$ , or streptavidin from the hybridization solution, Figure 6b–d spots show white-gray, light-orange, and orange color, respectively. When we compare images a and d in Figure 6, the order of the interference color of blue in Figure 6a is higher than the orange color in Figure 6d. This result shows that the biotin-streptavidin complexes lead to

an increase in the surface density and the disruption of the orientations of LC. Furthermore, the fluorescence intensity of DNA spots in Figure 6a ( $15847 \pm 499$ ) leads us to estimate the surface density of  $\text{T}_2/\text{biotin-P}_3/\text{SAv}$  complexes as  $1.05 \times 10^{12}/\text{cm}^2$ . By assuming one complex hybridized to one DNA probe on the surface, the hybridization efficiency is about 33%. Again, this brings us to conclude that the LC-based tool with the biotin-streptavidin complexes system is able to amplify the LC color contrast between ssDNA and the hybridized DNA–streptavidin complex, even at low hybridization efficiency.

When we compared with the Michel–Levy chart, the order of blue interference color is higher than that of the blue-orange color in Figure 5a.<sup>31</sup> This suggests that the disruption of the orientations of LC in Figure 6a is higher than Figure 5a. However, the fluorescence intensities for both spots in Figure 5a and 6a are  $15379 \pm 996$  and  $15847 \pm 499$ , respectively. This implies that the amount of streptavidin on the surface is about the same. When combined with the LC optical image, we can conclude that the higher interference color of Figure 6a is due to the branched-streptavidin complexes, which can disrupt the orientations of LC more significantly than the single-biotin-streptavidin conjugates.

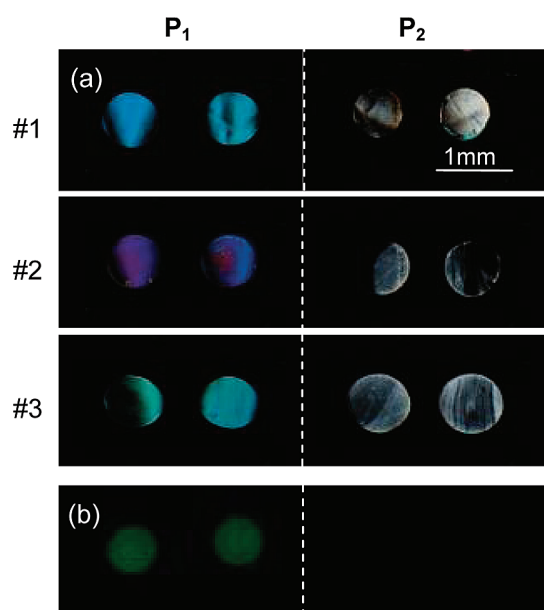


**Figure 7.** Specificity for DNA detection.  $P_1$  and  $P_2$  are complementary and non-complementary DNA probe to  $T_2$ , respectively. (a) LC images (in triplicates) showing  $P_1$  spots give blue or purple colors, whereas  $P_2$  spots give gray color. (b) Fluorescence image of the first sample confirms the successful hybridization of  $T_2$  to  $P_1$ .

**Specificity of Detection.** In view of the advantages of the application of LC on the branched-streptavidin complexes system, i.e., label-free detection and ability to distinguish ssDNA and dsDNA with high color contrast, we further explored the specificity of the branched-streptavidin complexes system in differentiating the complementary from the non-complementary DNA strands. We immobilized DNA probes  $P_1$  and  $P_2$  on solid surface and hybridized the probes to  $T_2$ /biotin- $P_3$ /SAV branched-streptavidin complexes.  $P_2$  probes are not complementary to  $T_2$  or biotin- $P_3$ . The experiment was repeated three times to test the reproducibility of the system. Triplicate results in Figure 7a show that  $P_1$  probes which are complementary to the complexes are in blue or purple color while  $P_2$  probes which are not complementary to the complexes are in white-gray color. This suggests that  $P_1$  spots have higher surface density than  $P_2$  spots, which is due to the specific hybridization of  $T_2$ /biotin- $P_3$ /SAV complexes to  $P_1$  but not  $P_2$ . The specificity of the detection is confirmed by the fluorescence image in Figure 7b, where only the  $P_1$  spots show green fluorescence signal from the Cy3-streptavidin (the fluorescence intensity of  $P_2$  spots was  $24 \pm 3$ ). On the basis of this information, we conclude that the  $P_1$  spots are in dsDNA-streptavidin complexes form while  $P_2$  spots remain as ssDNA. The hybridization is specific to the complementary DNA targets and LC-based detection tool combined with the branched-streptavidin complexes system can be used to specifically detect the complementary DNA targets on surface.

## CONCLUSIONS

We have shown that LC and its respective interference color could be used as a tool to detect the dsDNA on a solid surface. The introduction of single-biotin-streptavidin conjugates results in a higher surface density and better color contrast between ssDNA and dsDNA. An alternate approach is to form the branched-streptavidin DNA complexes prior to DNA hybridization. The

branched-streptavidin complexes system can give a more pronounced LC color contrast than single-biotin-streptavidin conjugates. It is able to detect the complementary DNA targets specifically. This LC-based method to detect DNA targets is the first step toward a simple, instrument-free, and high-throughput DNA detection method.

## ASSOCIATED CONTENT

**Supporting Information.** The indication of LC spot interference color. This material is available free of charge via the Internet at <http://pubs.acs.org>.

## AUTHOR INFORMATION

### Corresponding Author

\*E-mail: cheyk@nus.edu.sg.

## ACKNOWLEDGMENT

The work is funded by the Agency for Science and Technology Research (ASTAR) in Singapore under Project 082 101 0027

## REFERENCES

- (1) Kurian, K. M.; Watson, C. J.; Wyllie, A. H. *J. Pathol.* **1999**, *187*, 267–271.
- (2) Lockhart, D. J.; Winzler, E. A. *Nature* **2000**, *405*, 827–836.
- (3) Heller, M. J. *Annu. Rev. Biomed. Eng.* **2002**, *4*, 129–153.
- (4) Stears, R. L.; Martinsky, T.; Schena, M. *Nat. Med.* **2003**, *9*, 140–145.
- (5) Cheung, V. G.; Morley, M.; Aguilar, F.; Massimi, A.; Kucherlapati, R.; Childs, G. *Nature* **1999**, *21*, 15–19.
- (6) Pirrung, M. C. *Angew. Chem., Int. Ed.* **2002**, *41*, 1276–1289.
- (7) Heise, C.; Bier, F. F. *Top. Curr. Chem.* **2006**, *261*, 1–25.
- (8) Elhadj, S.; Singh, G.; Saraf, R. F. *Langmuir* **2004**, *20*, 5539–5543.
- (9) Bally, M.; Halter, M.; Voros, J.; Grandin, H. M. *Surf. Interface Anal.* **2006**, *38*, 1442–1458.
- (10) Gray, D. E.; Case-Green, S. C.; Fell, T. S.; Dobson, P. J.; Southern, E. M. *Langmuir* **1997**, *13*, 2833–2842.
- (11) Thiel, A. J.; Frutos, A. G.; Jordan, C. E.; Corn, R. M.; Smith, L. M. *Anal. Chem.* **1997**, *69*, 4948–4956.
- (12) Jordan, C. E.; Frutos, A. G.; Thiel, A. J.; Corn, R. M. *Anal. Chem.* **1997**, *69*, 4939–4947.
- (13) Gupta, V. K.; Skaife, J. J.; Dubrovsky, T. B.; Abbott, N. L. *Science* **1998**, *279*, 2077–2080.
- (14) Shah, R. R.; Abbott, N. L. *Science* **2001**, *293*, 1296–1299.
- (15) Tingey, M. L.; Wilyana, S.; Snodgrass, E. J.; Abbott, N. L. *Langmuir* **2004**, *20*, 6818–6826.
- (16) Clare, B. H.; Abbott, N. L. *Langmuir* **2005**, *21*, 6451–6461.
- (17) Kim, H.-R.; Kim, J.-H.; Kim, T.-S.; Oh, S.-W.; Choi, E.-Y. *Appl. Phys. Lett.* **2005**, *87*, 143901.
- (18) Bi, X.; Lai, S. L.; Yang, K.-L. *Anal. Chem.* **2009**, *81*, 5503–5509.
- (19) Xue, C.-Y.; Khan, S. A.; Yang, K.-L. *Adv. Mater.* **2009**, *21*, 198–202.
- (20) Lai, S. L.; Huang, S.; Bi, X.; Yang, K.-L. *Langmuir* **2009**, *25*, 311–316.
- (21) Chen, C.-H.; Yang, K.-L. *Langmuir* **2010**, *26*, 1427–1430.
- (22) Xue, C. Y.; Yang, K. L. *Langmuir* **2008**, *24*, 563–567.
- (23) Price, A. D.; Schwartz, D. K. *J. Am. Chem. Soc.* **2008**, *130*, 8188–8194.
- (24) Lai, S. L.; Hartono, D.; Yang, K.-L. *Appl. Phys. Lett.* **2009**, *95*, 153702.
- (25) Smith, C. L.; Milea, J. S.; Nguyen, G. H. *Top. Curr. Chem.* **2005**, *261*, 63–90.
- (26) Lai, S. L.; Chen, C.-H.; Yang, K.-L. *Langmuir* **2011**, *27*, 5659–5664.
- (27) Kahn, F. J. *Appl. Phys. Lett.* **1973**, *22*, 386–388.

- (28) Kocevar, K.; Musevic, I. *ChemPhysChem* **2003**, *4*, 1049–1056.
- (29) Lai, S. L.; Yang, K.-L. *Analyst* **2011**, DOI: 10.1039/c1an15173h.
- (30) Levicky, R.; Herne, T. M.; Tarlov, M. J.; Satija, S. K. *J. Am. Chem. Soc.* **1998**, *120*, 9787–9792.
- (31) Abramowitz, M.; Davidson, M. W. Michel-Levy Birefringence Chart. <http://micro.magnet.fsu.edu/primer/techniques/polarized/michel.html> (September 17).
- (32) Price, A. D.; Schwartz, D. K. *Langmuir* **2006**, *22*, 9753–9759.
- (33) Su, X.; Wu, Y.-J.; Robelek, R.; Knoll, W. *Langmuir* **2005**, *21*, 348–353.
- (34) Niemeyer, C. M.; Adler, M.; Pignataro, B.; Lenhert, S.; Gao, S.; Chi, L.; Fuchs, H.; Blohm, D. *Nucleic Acids Res.* **1999**, *27*, 4553–4561.
- (35) Niemeyer, C. M. *Angew. Chem., Int. Ed.* **2010**, *49*, 1200–1216.